InSight Aerothermal Environment Assessment

Robin A. S. Beck[1]
NASA Ames Research Center, Moffett Field, CA, 94035, USA

Jarvis T. Songer.[2]
Lockheed Martin Space, Littleton, CO, 80120, USA

Christine E. Szalai[3]
Jet Propulsion Laboratory, California Institute of Technology, Pasadena, CA, 91109, USA

David A. Saunders[4]
Analytical Mechanics Associates, Moffett Field, CA, 94035, USA

Mark A. Johnson[5]
Lockheed Martin Space, Littleton, CO, 80120, USA

Chris Karlgaard[6]
Analytical Mechanics Associates, Hampton, VA, 23666

The Mars Interior Exploration using Seismic Investigations, Geodesy and Heat Transport (InSight) spacecraft, which successfully touched down on the planet surface on November 26, 2018, was proposed as a near build-to-print copy of the Mars Phoenix vehicle to reduce the overall cost and risk of the mission. Since the lander payload and the atmospheric entry trajectory were similar enough to those of the Phoenix mission, it was expected that the Phoenix thermal protection material thickness would be sufficient to withstand the entry heat load. However, allowances were made for increasing the heatshield thickness because the planned spacecraft arrival date coincided with the Mars dust storm season. The aftbody Thermal Protection System (TPS) components were not expected to change. In a first for a US Mars mission, the aerothermal environments for InSight included estimates of radiative heat flux to the aftbody from the wake. The combined convective and radiative heat fluxes were used to determine if the as-flown Phoenix thermal protection system (TPS) design would be sufficient for InSight. Although the radiative heat fluxes on the aftbody were predicted to be comparable to, or even higher than the local convective heat fluxes, all analyses of the aftbody TPS showed that the design would still be adequate. Aerothermal environments were computed for the vehicle from post-flight reconstruction of the atmosphere and trajectory and compared

[1] Aerospace Engineer, Entry Systems and Vehicle Development Branch (TSS), AIAA Associate Fellow
[2] Aeronautical Engineer, Staff, Deep Space Exploration.
[3] Group Supervisor, EDL Systems & Advanced Technologies
[4] Senior Research Scientist, Aerothermodynamics Branch at NASA Ames Research Center, AIAA Senior Member
[5] Systems Engineer, Senior Staff, Deep Space Exploration
[6] Supervising Engineer, NASA Langley Research Center, AIAA Associate Fellow

with the design environments. These comparisons showed that the predicted as-flown conditions were less severe than the design conditions.

I. Introduction

The Interior Exploration using Seismic Investigations, Geodesy and Heat Transport (InSight) mission is a robotic lander designed to study the deep interior of the planet Mars. The primary instruments are intended to measure the seismic activities of Mars along with temperature distribution up to 6 meters in-depth. In order to reduce overall cost and risk of the mission, the InSight entry vehicle was designed to be a near build-to-print of the Phoenix entry vehicle, including the Thermal Protection System (TPS). Therefore, the baseline TPS design for the InSight entry vehicle included the same TPS materials and thicknesses as Phoenix. The aerothermal analysis of the InSight spacecraft was targeted to determine if the designed TPS thicknesses were sufficient to survive the InSight entry environments. Allowances were made for an increase in thickness for the TPS for the forebody due to a scheduled entry during the traditional dust storm season on Mars. Dust in the atmosphere was not expected to influence the convective heating on the aftbody other than the effects of slight increases in the density. Unlike Phoenix and all previous US Mars missions, this InSight mission included the radiative component of the heat flux on the spacecraft. All previous US Mars missions neglected the contribution of radiation to the total heating because it was believed to be negligible. At the time of InSight's project Critical Design Review (CDR), the InSight Aerothermal Working Group (AWG) began a radiation analysis effort based on recent theoretical analyses [1], simulations [2, 3, 4, 5, 6], experiments [7], and flight data [8] indicating that heating from mid-wave infrared CO_2 radiation would be significant, primarily on the aftbody components. This new approach influenced the prevailing TPS margin policy [9] by adding new uncertainties to the radiative heating [10]. All analyses showed that the design TPS thicknesses on the aftbody components had positive margins for the mission.

Immediately after the entry, descent, and landing of the InSight components on Mars on November 26, 2018, reconstruction of the entry began. Once the best estimated trajectory (BET) was determined [11, 12, 13], aerothermal analyses on that BET showed that the predicted as-flown conditions were more benign than the design conditions.

II. Aerothermal Design Analysis

The InSight geometry was a 70º sphere-cone forebody, and the aftbody consisted of a conical backshell and parachute cone, along with a parachute lid. The entry vehicle and TPS materials are illustrated in Fig. 1.

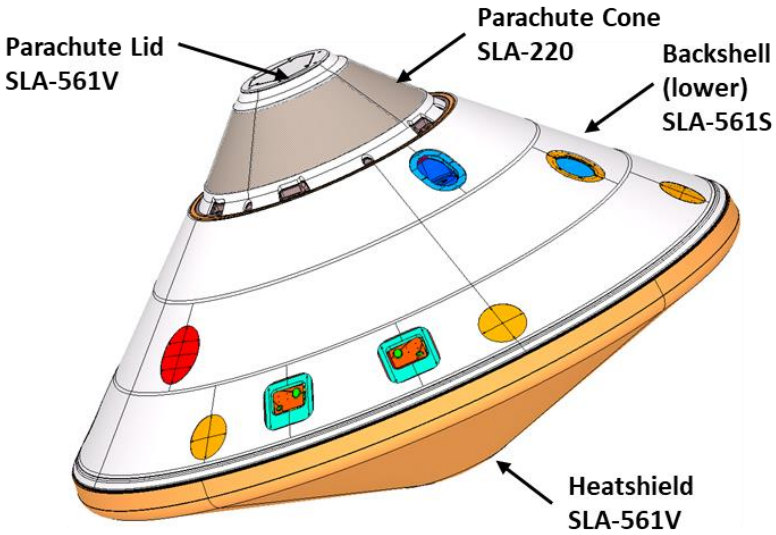

Fig. 1 InSight spacecraft geometry.

Design trajectories were determined from Monte Carlo simulations about the target trajectory. The trajectory designers provided the CFD analysts with synthetic trajectories that were created to bound the 99th percentile of the

ranges seen in the simulations. These bounding entries consisted of the trajectory that subjected the vehicle to the maximum heat rate (MHR) and the trajectory along which the vehicle would sustain the maximum total heat load (MHL). Analysts used the MHR trajectory to evaluate the survivability of the TPS materials and the MHL trajectory to determine the thickness of the TPS to keep the bond line temperatures below design allowables.

A. Convective Heating

Aerothermal convective heating calculations were performed at Lockheed Martin, using the LAURA code [20], and at NASA Ames Research Center, using the DPLR code [25]. Both codes are capable of calculating both 2-D/axisymmetric and full 3-D simulations. DPLR and LAURA are viewed as NASA's workhorse flow solvers and they have been extensively used to predict the aerothermal environments of planetary vehicles [14, 15, 16, 17, 18, 19].

The Langley Aerothermodynamic Upwind Relaxation Algorithm (LAURA) is a high fidelity, structured grid flow solver, specialized for hypersonic re-entry physics, utilizing state-of-the-art algorithms for CFD simulations [20, 21]. Key elements of LAURA include Roe's averaging [22] and Yee's Symmetric Total Variation Diminishing (STVD) [23] formulation of second-order, inviscid flux. Its non-equilibrium real-gas Navier-Stokes flow calculations are parallelized.

The Data Parallel Line Relaxation (DPLR) code uses a finite-volume discretization to solve the reacting Navier-Stokes equations for fluids in thermo-chemical non-equilibrium on structured grids. It is also parallelized for efficient computing on large clusters. While the software was originally designed for steady-state aerothermodynamic analysis of planetary entry vehicles, DPLR has evolved over the years to include a broad spectrum of numerical and physical models that enable it to accurately simulate most compressible flows. Additional details on DPLR's capabilities can be found in the references [24, 25, 26].

Both LAURA and DPLR were run with the Martian atmosphere modeled using a Mitcheltree 8-species (CO_2, CO, N_2, O_2, NO, C, N, O), 12 reaction model over a supercatalytic wall in radiative equilibrium. The InSight design trajectory was ballistic, although based on Phoenix trajectory reconstruction, some excursion from zero angle of attack was expected. While most of the aerothermal analyses were axisymmetric/2D, i.e., no angle of attack, additional 3D runs were performed with a 10^{o} angle of attack to assess the possible onset of turbulent flow on the heatshield.

Mars Science Laboratory (MSL) flight reconstruction [27] was used to determine updated, less conservative criteria for turbulent transition on the InSight heatshield. Based on the MSL data, InSight analysts used a momentum thickness Reynolds number criterion of Re_{θ}=400 for smooth wall transition onset and a roughness height Reynolds number criterion of Re_{kk}=200 for rough wall transition onset. Analysts determined an equivalent-sand-grain-roughness, k, by measuring the actual roughnesses on multiple SLA-561V arc jet test models and found that a value of 0.6 mm bounded all data on models tested in heat fluxes below 100 W/cm^2. Fully margined predicted heat fluxes on the InSight heatshield were substantially lower than 100 W/cm^2. Figure 2 shows the calculated values for Re_{θ} and Re_{kk} distributions along the InSight heatshield at various times in the trajectory flying at a 10^{o} angle of attack, including the peak heat flux time (PH) and the peak dynamic pressure times (PP). As seen in the figures, the values were substantially below the Re_{θ} = 400 and Re_{kk}=200 criteria. Therefore, analyses on the heatshield were performed with laminar flow.

The un-margined convective heating distributions calculated by both LAURA and DPLR are shown in Fig. 3. While LAURA and DPLR predict nearly identical results on the heatshield, there are some differences on the aftbody. Mid-lower backshell peak fluxes occurred inside regions of flow re-circulation with complex structure, where LAURA and DPLR solutions vary. The peaks were found at interfaces between "lobes." In order to be conservative when determining the TPS thickness requirements on the backshell, the analyses between the two codes were compared and the maximum values at each time were used to develop boundary conditions for thermal sizing analyses.

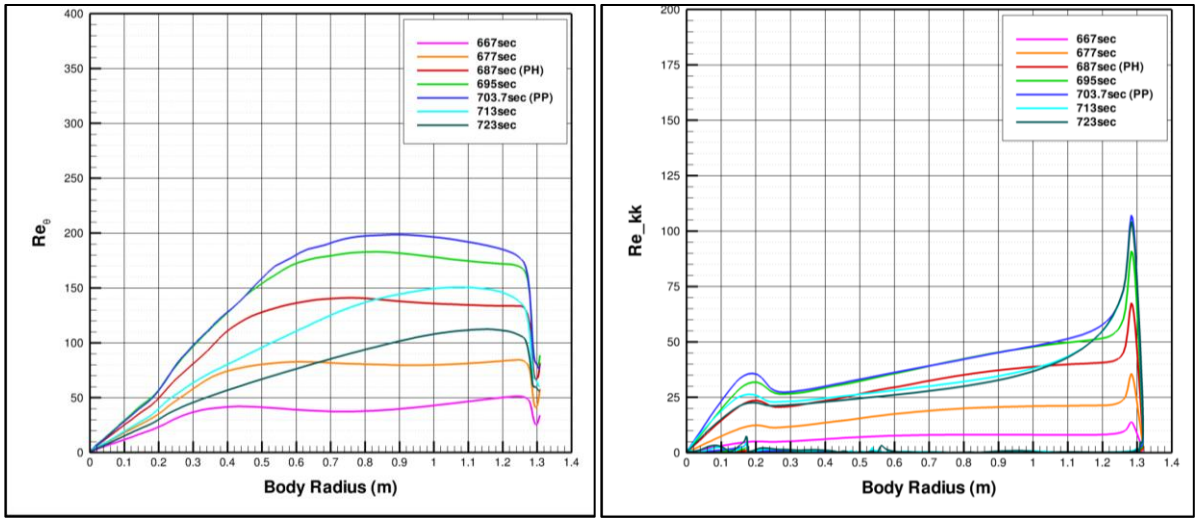

Fig. 2 Calculated Re_θ and Re_{kk} for the InSight heatshield at various times along the trajectory.

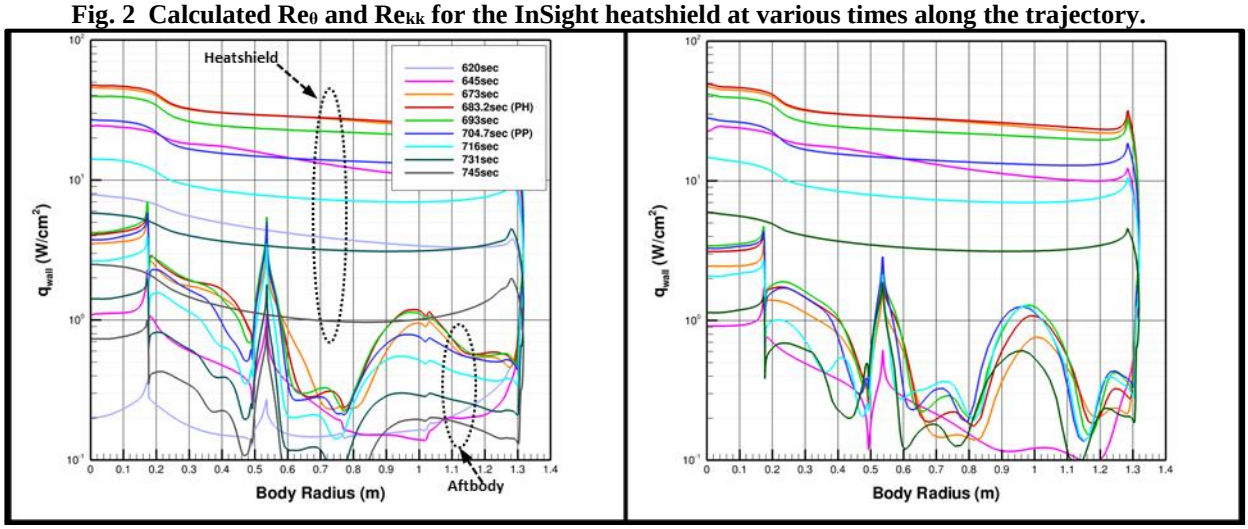

Fig. 3 Un-margined convective heat flux distribution on InSight at various times along the trajectory.

.

B. Radiative Heating

Early radiation analyses were performed by both LAURA/HARA and DPLR/NEQAIR. The High-temperature Aerothermodynamic RAdiation (HARA) model that was applied is discussed in detail by Johnston et al [28, 29]. A line-by-line approach is used for atoms and optically thick molecules, while a smeared band model is used for optically thin molecules. HARA's modeling is based on a set of atomic levels and lines from the National Institute of Standards and Technology (NIST) [30] and Opacity Project databases [31]. The atomic bound-free model is composed of cross sections from the Opacity project's online TOPbase [32], which were curve fit by Johnston [28]. HARA uses tangent-slab (1D assumption) as the default option for calculating the wall-directed radiative heat flux, with an option for running full angular integration for appropriate cases using a process known as ray tracing. Non-EQuilibrium AIR (NEQAIR) is a line-by-line radiation code which computes spontaneous emission, absorption and stimulated emission due to transitions between various energy states of chemical species along a line-of-sight. Twenty-two individual electronic transitions are considered for atoms and molecules, with the molecular band systems being resolved for each rotational line. Since the report of Whiting et al. [33], numerous updates have been incorporated into NEQAIR, including: using the latest version of the NIST atomic database (version 5.0) [34], using the bound-free cross sections from TOPbase [32], incorporating the CO_2 database from CDSD-4000 [1], parallelization, and improvements to the mechanics of QSS. The version of NEQAIR used preflight was v14.0.24. As with HARA, NEQAIR uses the tangent-slab approximation as the default option for radiation transport. For aftbody points, ancillary utilities enable NEQAIR to perform full hemispherical integration calculations of radiative heat flux comparable to HARA's ray tracing.

Early results showed significant differences between the solutions sets, due to inadequate resolution in the spectral grid in HARA that was later corrected [10]. For that reason, the DPLR/NEQAIR results formed the baseline solution for pre-flight, although sensitivity studies from LAURA/HARA and direct LAURA-DPLR and NEQAIR-HARA comparisons were also made.

For most of the pre-flight InSight calculations, NEQAIR was run in tangent-slab mode on axisymmetric flow solutions, as the traditional practice for radiation analysis in this work. Due to the complexities of the flow found in the wake of a vehicle, and the more complicated geometries on the aftbody, using a tangent-slab approximation is questionable for aftbody radiative heating calculations [6]. For more accurate estimation of radiative heat flux on the aftbody, full angular integrations are required. Full angular integration is achieved by performing a numerical integration of radiance at a body point with respect to solid angle over all possible lines of sight to/from the body point. While this approach has since been automated for both HARA and NEQAIR, pre-flight radiative conditions were evaluated with HARA ray tracing at few times and compared with the tangent-slab results. From these comparisons, conservative knock down factors for tangent slab values were developed for the various regions of the aftbody. Figure 4 shows the ratios of the ray tracing to the tangent-slab results over the entire body at the time of peak radiative heating on the parachute lid (left) and the time varying ratio on the parachute lid (right). Conservative knock down factors were determined, with the analysts using 1.0 (no reduction) for the mid lower backshell location, 0.75 for the main seal and parachute cone location, and 0.41 for the center of the parachute lid.

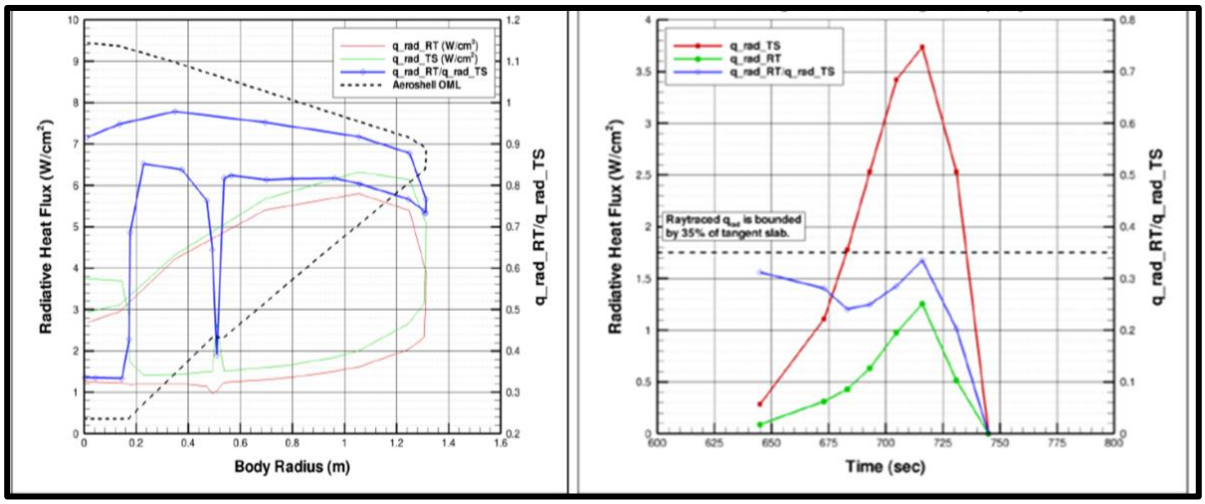

Fig. 4 Ratios of HARA ray tracing to tangent-slab radiation calculations.

C. Combined Aeroheating Results

Once the convective and radiative heating contributions were determined, they were combined to evaluate the effect of the radiative component on the total heating. For the heatshield stagnation point, Fig. 5 shows that the contribution of radiant heating was small and that convective heating dominated the total heating.

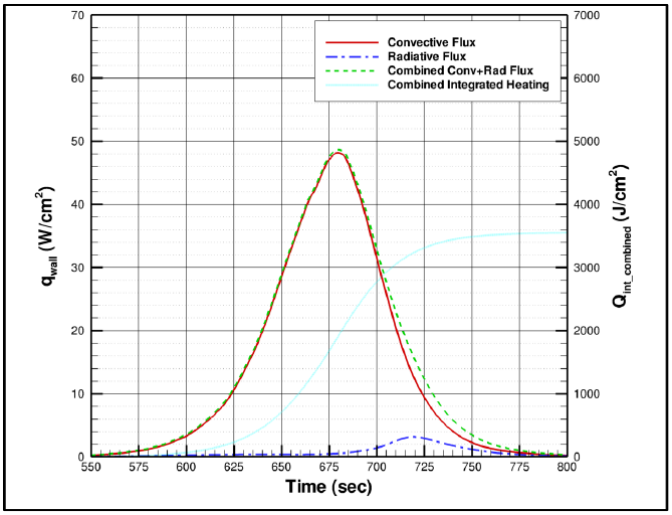

Fig. 5 Pre-flight predictions of the heatshield stagnation point heating.

Figures 6a, b, c, and d show the predicted convective and radiative heating for the main seal, mid lower backshell, the parachute cone, and the center of the parachute lid locations, respectively. Each of these locations was critical to determining the TPS thickness requirements. On the aftbody, several of the locations show the radiative heating to be at a similar magnitude to the convective heating. These results indicate that the previous approach to TPS design for Mars [9], neglecting radiative heating from the wake, could result in non-conservative designs for aftbody TPS.

Once the modeling uncertainties and margins (not discussed in this paper) were added to the design heating profiles, TPS thickness analyses were performed. The Phoenix aftbody TPS designs were found to be adequate for the InSight mission. The InSight heatshield TPS thickness was nevertheless augmented by about 25% for flight through a dusty atmosphere (also not discussed in this paper).

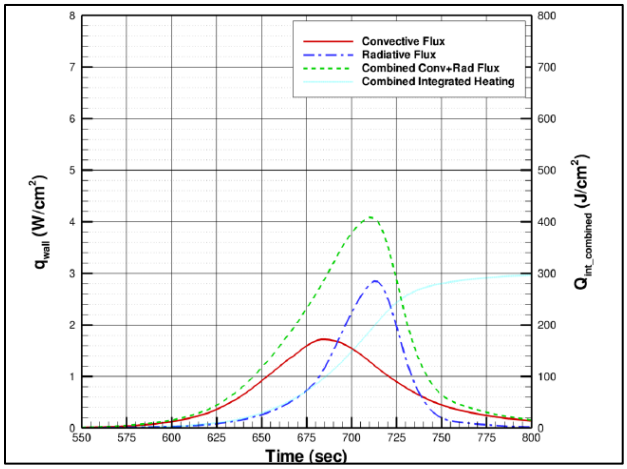

a) Main Seal heating

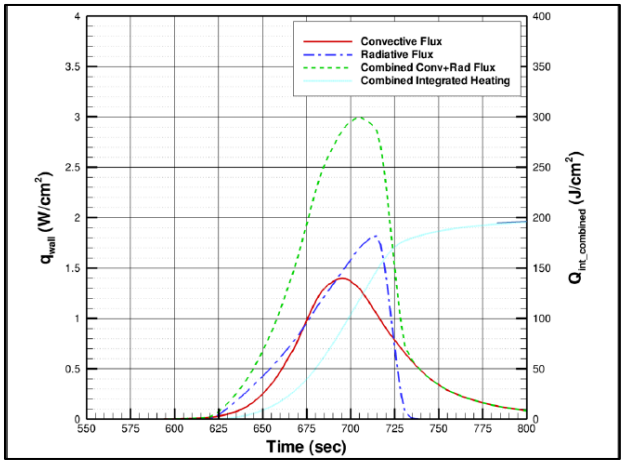

b) Mid Lower Backshell heating

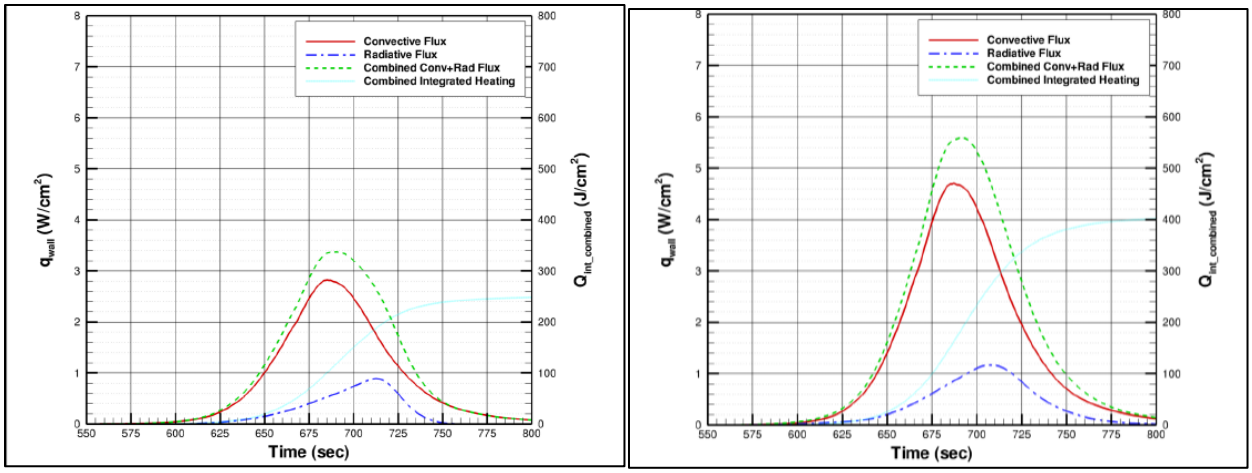

c) Parachute Cone Heating d) Parachute Lid Heating

Fig.6 Heating predictions for various locations on the InSight aftbody.

III. Reconstructed Aerothermal Environments

The InSight mission launched from Vandenberg AFB on May 5, 2018 and entered the atmosphere of Mars on November 26, 2018. Extensive data analyses were performed from all available instrumentation to reconstruct the best-estimated trajectory (BET) of the spacecraft. It should be noted that InSight did not have any aerothermal instrumentation (e.g. pressure sensors, heat flux gages, thermocouples), so aerothermal reconstruction predictions were based solely on the BET. Utilizing the BET, both DPLR and LAURA analyzed the convective heating on the vehicle with no angle of attack. As with pre-flight comparisons, both codes agreed within 1% on the forebody and had the expected differences on the aftbody. The LAURA code was run in 3-D to evaluate the conditions at angle of attack at the peak heating and peak pressure times. Boundary layer properties at angle of attack agreed with design analyses where the flow over the forebody remained laminar for the flight.

The BET reconstructed peak convective heating along the body for the InSight entry was predicted to be very similar to the MHL nominal values, as shown in Fig. 7 (red curves). The convective heating distribution at the peak dynamic pressure (Fig7, royal blue curves) was lower for the BET than the MHL design due to a faster entry duration.

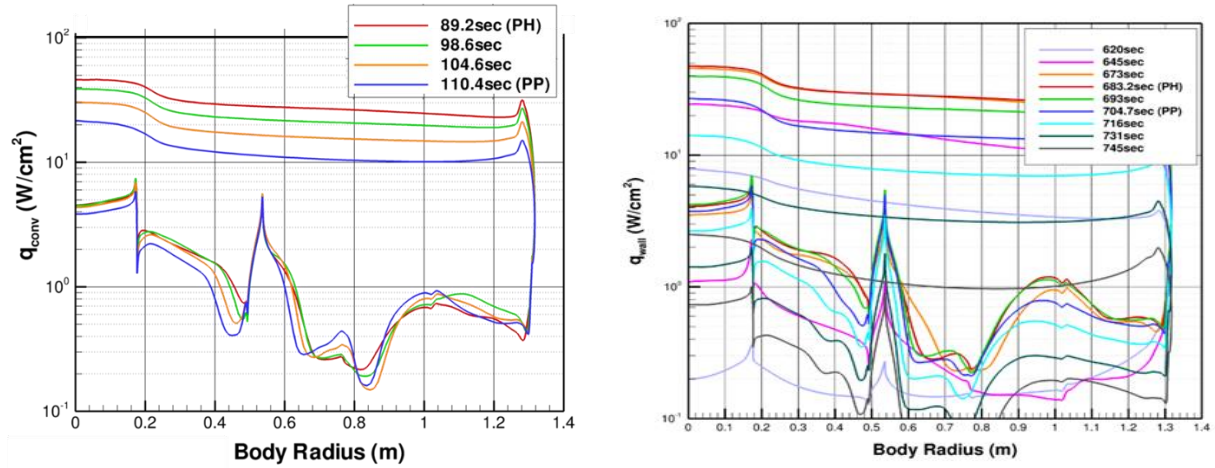

Fig. 7 Comparison of predicted convective heating profiles using the BET (left) and the MHL design trajectory (right).

The NEQAIR and HARA codes were used to analyze the radiative heating on the aftbody using full hemispherical integration. The codes agreed within 5% on most aftbody points of interest.

The aerothermal heating predictions for select locations for the BET are shown in Figs. 8 and 9.

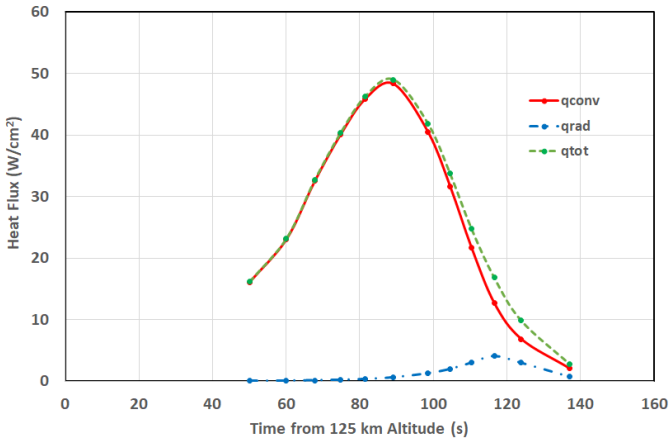

Fig. 8 Reconstructed stagnation point heating predictions for the BET.

Reconstruction has shown that the BET flew for a shorter time than the design environment as evident when comparing the stagnation point heating histories, shown in Fig. 10. The times for the MHL were adjusted such that the peak heating times coincide. While the predicted peak heat fluxes for the BET were similar to those for the MHL design, the predicted total heat loads on the vehicle were considerably less. Total heat load tends to drive the TPS thickness requirements. Therefore, the as-built TPS thicknesses were demonstrably conservative for the InSight as-flown trajectory.

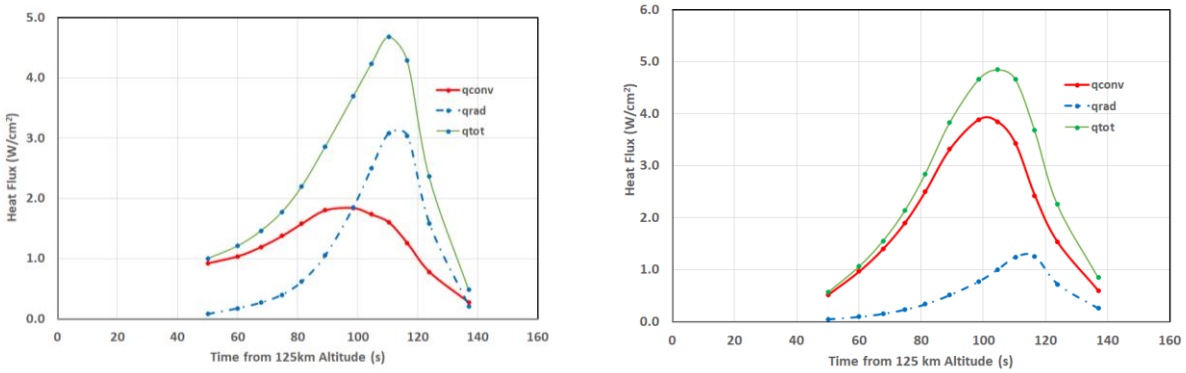

Fig. 9 Reconstructed heating predictions of the main seal (left) and parachute lid (right) for the BET.

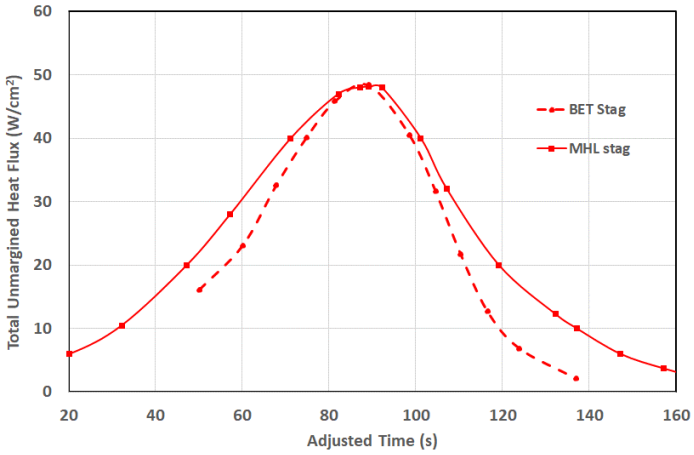

Fig. 10 Comparison of predicted BET and MHL stagnation point heating histories.

IV. Summary and Conclusions

The InSight mission was the first US mission to Mars to consider the radiative heating component on the backshell TPS. Although the preflight aerothermal analyses showed that the radiative heating on the heatshield was predicted to be extremely small, the analyses also showed that the radiative heating was predicted to be comparable to, and sometimes greater than, the convective heating for several aftbody locations. This should be further verified when the Mars 2020 spacecraft enters the Mars atmosphere in February 2021 with aftbody total heat flux and radiometer measurements from the MEDLI2 set of instruments [35]. As NASA proceeds with future Mars missions, the aftbody radiation will no longer be neglected when designing the TPS for the spacecraft.

Acknowledgments

The authors would like to acknowledge the NASA Space Technology Mission Directorate for sponsoring the InSight post-flight reconstruction efforts.

References

[1] Tashkun, S. and Perevalov, V., "CDSD-4000: High-Resolution, High-Temperature Carbon Dioxide Spectroscopic Data-bank," *Journal of Quantitative Spectroscopy and Radiative Transfer*, Vol. 112, No. 9, 2011, pp. 1403-1410.

[2] Babou, Y., Riviere, P., Perrin, M.-Y., and Soufiani, A., "Spectroscopic data for the prediction of radiative transfer in CO_2-N_2 plasmas," *Journal of Quantitative Spectroscopy and Radiative Transfer*, Vol. 110, No. 1-2, 2009, pp. 89 - 108.

[3] da Silva, M. L. and Beck, J., "Contribution of CO_2 IR Radiation to Martian Entries Radiative Wall Fluxes," *49th AIAA Aerospace Sciences Meeting and Exhibition*, 2011. AIAA Paper 2011-135.

[4] LeBrun, A. and Omaly, P., "Investigation of Radiative Heat Fluxes for EXOMARS Entry in the Martian Atmosphere," 4th International Workshop on Radiation of High Temperature Gases in Atmospheric Entry, 2010.

[5] Palmer, G. and Cruden, B., "Experimental Validation of CO_2 Radiation Simulations," *43rd AIAA Thermophysics Conference*, New Orleans, Louisiana, 2012, AIAA Paper 2012-3188.

[6] Mazaheri, A., Johnston, C., and Sefidbakht, S., "Three-Dimensional Radiation Ray Tracing for Shock-Layer Radiative Heating Simulations," *Journal of Spacecraft and Rockets*, Vol. 50, No. 3, 2013, pp. 485-493.

[7] Cruden, B., Prabhu, D., and Brandis, A., "Measurement and Characterization of Mid-wave Infrared Radiation CO_2 Shocks," *11th AIAA/ASME Joint Thermophysics and Heat Transfer Conference*, Atlanta, Georgia, 2014, AIAA Paper 2014-2962.

[8] Cruden, B., Brandis, A., White, T., Mahzari, M., & Bose, D., "Radiative Heating for MSL Entry: Verification of Simulations from Ground Test to Flight Data," *AIAA SciTech Conference*, Kissimee, Florida, 2015, AIAA Paper 2015-1894.

[9] Cozmuta, I., Wright, M., Laub, B., and Willcoxson, W., "Defining Ablative Thermal Protection System Margins for Planetary Entry Vehicles," *42nd AIAA Thermophysics Conference*, Honolulu, HI, 2011, AIAA Paper 2011-3757.

[10] Brandis, A., Saunders, D., Johnston, C., Cruden, B., White, T., "Radiative Heating on the Aftbody of Martian Entry Vehicles," *45st AIAA Thermophysics Conference*, Dallas, Texas, 2015, AIAA Paper 2015-3111.

[11] Maddock, R., "InSight EDL Reconstructed Performance vs. Final Operational Prediction," *SciTech Forum*, Orlando, Florida 2020, AIAA Paper 2020-****

[12] Karlgaard, C. "Atmosphere Reconstruction of InSight EDL", *SciTech Forum*, Orlando, Florida 2020, AIAA Paper 2020-****

[13] Korzun, A., "Aerodynamics Reconstruction and Reconciliation of InSight EDL", *SciTech Forum*, Orlando, Florida 2020, AIAA Paper 2020-****

[14] Edquist, K. T., Dyakonov, A. A., Wright, M. J., Tang, C. Y., "Aerothermodynamic Environments Definition for the Mars Science Laboratory Entry Capsule," *45th AIAA Aerospace Sciences Meeting and Exhibit*, Reno, Nevada, AIAA Paper 2007-1206.

[15] Wright, M. J., Prabhu, D. K., and Martinez, E. R., "Analysis of Afterbody Heating Rates on the Apollo Command Module, Part 1: AS-202," *AIAA Thermophysics Conference*, Portland, OR, June 2004. AIAA Paper No. 2004-2456,

[16] Wright, M. J., Loomis, M. A., and Papadopoulos, P. E., "Aerothermal Analysis of the Project Fire II Afterbody Flow," *Journal of Thermophysics and Heat Transfer*, Vol. 17, No. 2, 2003, pp. 240-249.

[17] Papadopoulos, P., Prabhu, D., Olynick, D., Chen, Y. K., and Cheatwood, F. M., "CFD Code Validation and Comparisons for Mars Entry Simulations," *AIAA Aerospace Sciences Meeting and Exhibit*, Reno, NV, January 1998. AIAA Paper 98-0272

[18] Queen, E. M., Cheatwood, F. M., Powell, R. W., Braun, R. D., and Edquist, C. T., "Mars Polar Lander Aerothermodynamic and Entry Dispersion Analysis," *Journal of Spacecraft and Rockets*, Vol. 36, No. 3, May-June 1999.

[19] Gnoffo, P. A., Weilmuenster, K. J., Braun, R. D., and Cruz, C. I., "Influence of Sonic-Line Location on Mars Pathfinder Probe Aerothermodynamics," *Journal of Spacecraft and Rockets*, Vol. 33, No. 2, March-April 1996.

[20] Mazaheri, A., Gnoffo, P., Johnston, C., and Kleb, B., "LAURA Users Manual," Technical Report. NASA TM 2010-216836, 2010.

[21] Gnoffo, P., Gupta, R., and Shinn, J., "Conservation Equations and Physical Models for Hypersonic Air Flows in Thermal and Chemical Nonequilibrium," Technical Report. NASA TP-2867, 1989.

[22] Roe, P., "Approximate Riemann Solvers, Parameter Vectors, and Difference Schemes," *Journal of Computational Physics*, Vol. 43, No. 2, 1981, pp. 357-372.

[23] Yee, H. C., "A Class of High-Resolution Explicit and Implicit Shock Capturing Methods," NASA TM 101088,
[24] February 1989.
[25] Wright, M., A Family of Data-Parallel Relaxation Methods for the Navier-Stokes Equations, Ph.D. thesis, University of Minnesota, 1997.
[26] Wright, M., Candler, G., and Bose, D., "Data-Parallel Line Relaxation Method for the Navier-Stokes Equations," *AIAA Journal*, Vol. 36, No. 9, 1998, pp. 1603-1609.
[27] Wright, M., White, T., and Mangini, N., "Data-Parallel Line Relaxation (DPLR) Code User Manual Acadia-Version 4.01.1," NASA/TM-2009-215388, NASA Ames Research Center, October 2009
[28] White, T., Mahzari, M., Bose, D, Santos, J. "Post-flight Analysis of the Mars Science Laboratory Thermal Protection System Response," *44th AIAA Thermophysics Conference*, San Diego, CA, June 2013. AIAA Paper 2013-2779
[29] Johnston, C., Hollis, B., and Sutton, K., "Spectrum Modeling for Air Shock-Layer Radiation at Lunar-Return Conditions, *Journal of Spacecraft and Rockets*, Vol. 45, No. 5, 2008, pp. 865-878.
[30] Johnston, C. O., Hollis, B., and Sutton, K., "Non-Boltzmann Modeling for Air Shock Layers at Lunar Return Conditions," *Journal of Spacecraft and Rockets*, Sep.-Oct. 2008.
[31] Ralchenko, Y., "NIST Atomic Spectra Database, Version 3.1.0," https://www.nist.gov/pml/atomic-spectra-database , July 2006, last accessed September 3rd, 2007.
[32] The Opacity Project Team, *The Opacity Project*, Vol. 1, Bristol and Philadelphia: Institute of Physics Publishing, 1995.
[33] Cunto, W., Mendoza, C., Ochsenbein, F., and Zeippen, C., "TOPbase at the CDS," *Astronomy and Astrophysics*, Vol. 275, Aug. 1993, pp. L5-L8. see also http://cdsweb.u-strasbg.fr/topbase / topbase.html
[34] Whiting, E., Park, C., Yen, L., Arnold, J., and Paterson, J., "NEQAIR96, Nonequilibrium and Equilibrium Radiative Transport and Spectra Program: User's Manual," Technical Report NASA RP-1389, Ames Research Center, Moffett Field, 1996.
[35] Kramida, A., Ralchenko, Y., Reader, J., and Team, N. A., "NIST Atomic Spectra Database, Version 5.0.0" https://www.physics.nist.gov/asd/ , July 2012, last accessed July, 2012
[36] Hwang, H., Bose, D., Wright, H., White, T., Schoenenberger, M., Santos, J., Karlgaard, C., Oishi, T., and Trombetta, D., "Mars 2020 Entry, Descent, and Landing Instrumentation (MEDLI2)," *46th AIAA Thermophysics Conference*, Washington, D.C., June 2016. AIAA Paper 2016-3536